Deposition of Mercury in Forests Across a Montane Elevation Gradient: Elevational and Seasonal Patterns in Methylmercury Inputs and Production

Authors: Jacqueline R Gerson,[123] Charles T Driscoll,[1] Jason D Demers,[4] Amy K Sauer,[5] Bradley D Blackwell,[6] Mario R Montesdeoca,[1] James B Shanley,[7] and Donald S Ross[8]

[1] Department of Civil and Environmental Engineering, Syracuse University
[2] Current Affiliation: University Program in Ecology, Department of Biology, Duke University
[3] Corresponding Author: 732-710-1844, jgerson1@gmail.com
[4] Department of Earth and Environmental Sciences, University of Michigan
[5] Biodiversity Research Institute
[6] Environmental Protection Agency Gulf Ecology Division
[7] U.S. Geological Survey
[8] Department of Plant and Soil Science, University of Vermont

This is the author manuscript accepted for publication and has undergone full peer review but has not been through the copyediting, typesetting, pagination and proofreading process, which may lead to differences between this version and the Version of Record. Please cite this article as doi: 10.1002/2016JG003721

Index Terms: Bioavailability: chemical speciation and complexation, Biogeochemical cycles, Metals, Soils/pedology, Trace element cycling

Keywords: Adirondacks, Deposition, Forests, Mercury, Methylmercury, Mountain

Abstract

Global mercury contamination largely results from direct primary atmospheric and secondary legacy emissions, which can be deposited to ecosystems, converted to methylmercury, and bioaccumulated along food chains. We examined organic horizon soil samples collected across an elevational gradient on Whiteface Mountain in the Adirondack region of New York State, USA to determine spatial patterns in methylmercury concentrations across a forested montane landscape. We found that soil methylmercury concentrations were highest in the mid-elevation coniferous zone (0.39 ± 0.07 ng/g) compared to the higher elevation alpine zone (0.28 ± 0.04 ng/g) and particularly the lower elevation deciduous zone (0.17 ± 0.02 ng/g), while the percent of total mercury as methylmercury in soils decreased with elevation. We also found a seasonal pattern in soil methylmercury concentrations, with peak methylmercury values occurring in July. Given elevational patterns in temperature and bioavailable total mercury (derived from mineralization of soil organic matter), soil methylmercury concentrations appear to be driven by soil processing of ionic Hg, as opposed to atmospheric deposition of methylmercury. These methylmercury results are consistent with spatial patterns of mercury concentrations in songbird species observed from other studies, suggesting that future declines in mercury emissions could be important for reducing exposure of mercury to montane avian species.

Key Points

- Total mercury and methylmercury concentrations and fluxes are examined across an elevational gradient on an Adirondack, NY mountain
- Methylmercury concentrations across the elevational gradient are greatest in mid-elevation coniferous zones
- Soil methylmercury concentrations are driven by the internal processing of mercury, rather than external inputs of methylmercury

1. Introduction

Mercury (Hg) is a potent neurotoxin that impacts the health of both humans and wildlife, even in remote areas [*Driscoll et al.*, 2007; *Evers et al.*, 2007]. Atmospheric deposition of Hg has increased nearly 3.5 times since industrialization, primarily as a result of anthropogenic activities [*Fitzgerald et al.*, 1998; *Lorey and Driscoll*, 1999; *Driscoll et al.*, 2013]. Total Hg (THg) enters ecosystems via wet (precipitation and cloudwater) or dry deposition, with inputs varying by forest cover type and atmospheric Hg speciation [*Blackwell et al.*, 2014]. Dry deposition can occur as the adsorption of reactive gaseous Hg (RGM, Hg^{2+}) and particulate Hg (PHg) to the leaf surface [*Lovett and Lindberg*, 1984; *Rea et al.*, 2000, 2001]. Mercury from dry deposition can enter soils via throughfall, which leaches Hg from the leaf surface [*Choi et al.*, 2008; *Fu et al.*, 2010]. Additionally, Hg can enter forested ecosystems via absorption of gaseous elemental Hg (GEM, Hg^{o}) from the atmosphere through the stomata of canopy foliage, followed by deposition to the soil in litterfall [*Rea et al.*, 2000, 2002; *Graydon et al.*, 2008; *Rutter et al.*, 2011; *Risch et al.*, 2012; *Demers et al.*, 2013]. Many studies have found litterfall to be the dominant input of THg to deciduous forest ecosystems. Conversely, coniferous forests have higher throughfall THg deposition than deciduous forests due to a greater scavenging efficiency driven by waxy cuticles, surface roughness, and high leaf surface area [*Kolka et al.*, 1999; *Rea et al.*, 2002; *Demers et al.*, 2007; *Johnson et al.*, 2007; *Bushey et al.*, 2008; *Graydon et al.*, 2008; *Fisher and Wolfe*, 2012; *Blackwell et al.*, 2014]. Methyl Hg (MeHg), the form of Hg that drives human and wildlife exposure, has the potential to form abiotically in the atmosphere via

oxidative methylation of Hg or decomposition of dimethyl Hg or to enter the atmosphere via evasion from terrestrial or aquatic ecosystems [*Conaway et al.*, 2010; *Fu et al.*, 2010]. This atmospherically-derived MeHg can then be deposited onto the landscape via the same pathways as THg. However, atmospheric processes of MeHg formation and transport are typically limited, and most MeHg is believed to be produced directly within terrestrial or aquatic ecosystems [*Grigal*, 2003].

While many studies have examined the transport and fate of Hg in the environment, most have focused on aquatic ecosystems since MeHg bioaccumulation in fish is the dominant transfer pathway to humans [*Dellinger et al.*, 2012]. Nevertheless, MeHg bioaccumulation also occurs in terrestrial ecosystems, potentially due to the importance of nearby aquatic macroinvertebrates; several studies have identified high Hg concentrations in terrestrial songbirds, invertebrates, and land biota, while other research has documented altered physiological, behavioral, and reproductive functions in wildlife populations resulting from exposure to elevated high MeHg concentrations [*Rimmer et al.*, 2005; *Evers et al.*, 2007; *Townsend et al.*, 2014]. While it is evident that MeHg concentrations increase with higher trophic levels [*Rimmer et al.*, 2010], the pathway of Hg from the atmosphere and supply of MeHg to terrestrial biota are not fully understood. In fact, though several forested mountain environments in the northeastern United States (including the Adirondacks) have been identified as "biological Hg hotspots" [*Evers et al.*, 2007], these classifications are based predominantly upon the contamination of aquatic ecosystems due to limited observations for terrestrial ecosystems.

Previous studies have shown that once Hg has been deposited, soils act as a net sink for Hg and a source of MeHg [*Hojdová et al.*, 2007]. Methyl Hg is produced in soils predominantly by sulfate reducing and iron reducing bacteria under reducing conditions [*Compeau and Bartha*, 1985], though investigations have also shown the methylation of Hg by other bacteria (such as iron reducing bacteria) that also contain the hgcAB gene pair [*Kerin et al.*, 2006; *Gilmour et al.*, 2013; *Podar et al.*, 2015]. Storage capacity of Hg within soils is enhanced by organic matter (OM) content, but the exact role of elevation remains poorly characterized [*Yu et al.*, 2011; *Townsend et al.*, 2014]. Based upon soil characteristics, tree species, precipitation patterns, and expected Hg inputs, ecosystems at higher elevations are thought to receive higher Hg deposition and support greater methylation [*Lawson et al.*, 2003; *Yu et al.*, 2014]. Findings of increased Hg concentrations in invertebrates, salamanders, and birds [*Blais et al.*, 2006; *Townsend et al.*, 2014], along with higher concentration of other contaminants [*Reiners et al.*, 1975; *Lovett and Kinsman*, 1990; *Miller et al.*, 1993; *Lawson et al.*, 2003], with increases in elevation support this hypothesis. Moreover, several studies have also reported higher concentrations of soil THg in coniferous stands compared to deciduous forests [*Kolka et al.*, 1999; *Graydon et al.*, 2008; *Fisher and Wolfe*, 2012]. Given that coniferous trees are often found at higher elevations, this forest cover type may also contribute to higher concentrations of Hg in sub-alpine zones. Nonetheless, to our knowledge, no studies have investigated forest ecosystem MeHg concentrations, fluxes, or pools along an elevational gradient.

In this study, we seek to understand the inputs and fate of THg and MeHg in a montane forested ecosystem of the Adirondack region in New York State. To achieve this objective, open precipitation, cloudwater, throughfall, litterfall, and soil samples were examined across a 1000 m elevational gradient on Whiteface Mountain throughout the growing season (May-September). Specifically, our research questions are: 1) What are the relative contributions of the major sources of THg and MeHg to the forest ecosystem?; 2) How do THg and MeHg concentrations, fluxes, and pools vary across an elevational gradient and among different forest cover types (deciduous, coniferous, alpine)?; 3) How do THg and MeHg concentrations, fluxes, and pools vary across the growing season (May-September)?

2. Materials and Methods

2.1 Study Area and Sample Plots

Whiteface Mountain is in the northeastern Adirondacks of New York State (44.37°N, 73.90°W at the summit; Figure A1). With a summit elevation of 1483 m, it is the fifth highest peak in the Adirondacks, and the most westerly peak of the 46 High Peaks in the region. Atmospheric chemistry and physics as well as forest ecology have been monitored at Whiteface Mountain since the 1980s as part of the State University of New York at Albany Atmospheric Science Research Center [ASRC; *Lovett and Kinsman*, 1990; *Miller et al.*, 1993; *Dukett et al.*, 2011]. Atmospheric monitoring stations are located at 610 m and at the summit, and cloudwater collection occurs at the summit. Both stations on Whiteface Mountain are managed by the New

York State Department of Environmental Conservation (NYSDEC) as part of the Clean Air Status and Trends Network (CASTNet) and National Atmospheric Deposition Program National Trends Network (NADP NTN). There are two Mercury Deposition Network (MDN) sites nearby at Huntington Forest in the Adirondacks (NY20, 50 km distance) and Underhill, VT (VT99, 80 km distance).

Forest communities on Whiteface Mountain consist of three major zones: deciduous, coniferous, and alpine [*Miller et al.*, 1993; *Blackwell and Driscoll*, 2015]. The deciduous forest zone is located at low elevations of 400 to 900 m, has a mean canopy height ranging from 8.3 to 11.8 m, and is dominated by sugar maple (*Acer saccharum*), yellow birch (*Betula alleghaniensis*), red maple (*Acer rubrum*), and American beech (*Fagus grandifolia*). The coniferous forest zone is located at mid-elevations of 1000 to 1300 m, has a mean canopy height ranging from 6.0 to 8.1 m, and is dominated by balsam fir (*Abies balsamea*) and red spruce (*Picea rubens*). The alpine forest zone is located at high elevations of 1350 m to the summit at 1483 m, has a mean canopy height generally less than 2 m, and is dominated by sparse, krummholz-form balsam fir mixed with alpine tundra. Across Whiteface Mountain, the maximum mean canopy height occurs at 825 m and decreases linearly at higher elevations [*Miller et al.*, 1993]. Leaf area index (LAI) reaches its maximum at low- to mid-elevation (800 to 1220 m).

Fifteen plots were established in 2010 and 2015 across an elevational gradient on the eastern slope of Whiteface Mountain. Plot location, sample collection methodology, and sample

analysis are described in Blackwell and Driscoll (2015). Five plots were established within each forest cover type: four plots under the canopy (twelve total canopy plots) and one in an open area (three total open plots). The four under-canopy plots were equally spaced by elevation within each forest cover type.

2.2 Sample Collection

Soil samples were previously obtained in June, July, and September 2010 from twelve canopy plots, as described in Blackwell and Driscoll (2015). Soil samples were collected with a split-PVC corer and divided visually into Oi/Oe (containing slightly decomposed leaf litter and organic matter) and Oa (highly decomposed organic matter) horizons. In 2015, litterfall was collected from each canopy plot in two plastic mesh-lined crates that were deployed in May and retrieved in October. This relatively long deployment period could potentially result in some retention of throughfall Hg by deposited litter [*Demers et al.*, 2007]. However, deciduous litterfall largely occurs during a short period at the end of the growing season, and coniferous litterfall occurs throughout the year; the applied deployment period was used to collect coniferous litter over the growing season. Samples were handled with clean nitrile gloves, placed in plastic bags, transported on ice to the laboratory, and frozen until processed.

Throughfall and open precipitation samples were collected monthly from May through September 2015 at each canopy and open plot, respectively. Two sample trains were established in the field: one for Hg analyses and one for ancillary chemical analyses (dissolved organic

carbon [DOC] and sulfate [SO_4^{2-}]), with each open plot containing duplicate Hg sample trains. Mercury sampling trains were placed at plots and collected monthly using the clean hands-dirty hands protocol (EPA Method 1669). Briefly, Hg sample trains consisted of a glass funnel connected to two 500 mL Teflon bottles via perfluoroalkoxy (PFA) tubing and styrene-ethylene-butadiene-styrene (SEBS) block polymer (C-Flex) tubing with a loop as a vapor lock. Glass funnels contained glass wool to prevent debris and insects from entering the sample train. Prior to deployment, glass funnels, PFA tubing, and Teflon bottles were pre-rinsed with 18.2 MΩcm Milli-Q water, immersed for a minimum of 24 hours in 10% nitric acid (HNO_3), rinsed three times with 18.2 MΩcm Milli-Q water, allowed to dry in a clean room, and double-bagged. Teflon bottles were stored until deployment with 10% trace metal grade hydrochloric acid (HCl) containing less than 0.1% Hg. At the time of deployment, all 500 mL Teflon bottles were acidified with two mL of trace metal grade HCl. C-flex tubing used to connect the glass funnels with the PFA tubing were pre-washed six times with 18.2 MΩcm Milli-Q water. New pre-rinsed C-flex tubing and glass wool were utilized at each deployment. Each Hg sampling train was replaced monthly at the time of sample collection. Teflon bottles were double-bagged, transported to Syracuse University, and stored at 4°C until analysis. Laboratory blanks (n=4) of the Hg sampling train had THg concentrations below the detection limit, and sample train standard spikes (5 ng/L) had recoveries of 90-110%. Ancillary chemistry sample trains consisted of a polyethylene funnel connected to a 1L polyethylene bottle via polyvinyl chloride tubing and C-flex tubing with a loop as a vapor lock. Prior to deployment, plastic funnels and one L bottles

were pre-rinsed with deionized water, filled overnight with 10% HCl, and rinsed six times with deionized water. Polyvinyl chloride tubing was rinsed six times with deionized water. Mercury and ancillary chemistry method blanks were collected during each deployment.

Cloudwater was collected at the summit of Whiteface Mountain during 22 precipitation-free cloud events from July through September 2015. Cloudwater was collected with a passive sampler consisting of a Teflon-coated steel cartridge strung with 0.035 inch Teflon filament that condensed cloud water and mounted on the roof of the facility. Each sample was collected in a polypropylene funnel lined with Teflon and connected to a 500 mL polyethylene terephthalate copolyester glycol (PETG) bottle via PFA tubing. The sampler was housed between sampling events in a PVC pipe lined with Teflon and covered with a stainless steel cap. Prior to the first deployment, Teflon strings and PFA tubing were pre-rinsed with 18.2 MΩcm Milli-Q water, immersed for a minimum of 24 hours in 10% HNO_3, rinsed three times with 18.2 MΩcm Milli-Q water, allowed to dry in a clean room, and double-bagged. Samples were acidified to 0.4% using trace metal grade HCl, transported to Syracuse University, and stored at 4°C until analysis.

2.3 Laboratory Analyses: Soil and Litterfall Samples

Of the 216 soil samples, 95% were previously analyzed for THg, percent carbon (%C), and percent nitrogen (%N), as reported in Blackwell and Driscoll (2015). We have completed THg analyses on all samples, as well as performed MeHg and percent sulfur (%S) analyses on all 2010 soil samples (n=216). Litterfall samples (n=24) were analyzed for THg, %C, %N, and %S.

Soil samples and litterfall samples were freeze-dried to a constant weight and analyzed for THg with a Leco AMA 254 via thermal decomposition, catalytic reduction, amalgamation, desorption, and atomic absorption spectroscopy (EPA Method 7473). The instrument was calibrated using National Institute of Standards and Technology (NIST) certified reference material 1633b (coal fly ash, 143 ng/g) and Canadian National Research Council (CNRC) certified reference material MESS-3 (marine sediment, 91 ng/g) with a detection limit of 0.2 ng Hg. Continuous calibration verification (CCV) and matrix spikes (MS) were performed using NIST 1633b, and quality control standard (QCS) was performed using MESS-3. For MeHg analyses, soil samples were microwave digested with trace metal grade HNO_3 and frozen until analysis [*Tseng et al.*, 1997; *Rahman and Kingston*, 2005]; litterfall samples were digested with 2% potassium hydroxide in methanol at 55°C for a minimum of 48 hours [*Hall and St. Louis*, 2004; *Hintelmann and Nguyen*, 2005; *Yu et al.*, 2010]. Digested samples were analyzed via direct aqueous ethylation with sodium tetraethylborate, purge and trap, and cold vapor atomic fluorescence spectroscopy (CVAFS, EPA Method 1630) on a Tekran 2500 spectrometer. Calibration, CCV, on-going precision and recovery (OPR), laboratory control standard (LCS), MS, and method detection limit (MDL) were performed using Frontier Geosciences certified laboratory MeHg standards. For soil samples, QCS was performed using ERM-580 (estuarine sediment, 75.5 ng/g). For litterfall samples, QCS was performed using TORT-2 (lobster hepatopancreas, 270 ng/g).

Percent C, %N, and %S were measured on freeze-dried soil and litterfall samples with a Costech 4010 Elemental Analyzer. Calibration and CCV for %C and %N analyses were performed using acetanilide (10.36% N, 71.09% C), and QCS was performed using atropine (4.84% N, 70.56% C). NIST certified reference sample 2709 (San Joaquin soil, 1.40% C) was used as an external standard for %C, and NIST 1515 was used as an external standard for %N (apple leaves, 2.25% N). Calibration and CCV for %S analyses were performed using sulfanilamide (18.62% S), and QCS was performed using BBOT (7.44% S). NIST 1515 (apple leaves, 0.18% S) was used as an external standard. All quality control results for Hg and ancillary chemistry can be found in Supplementary Table A1.

2.4 Laboratory Analyses: Throughfall, Open Precipitation, and Cloudwater Samples

Throughfall (n=57) and open precipitation samples (n=15) were analyzed for THg, MeHg, SO_4^{2-}, and DOC. Cloudwater samples (n=22) were analyzed for MeHg and THg. Throughfall, precipitation, and cloudwater samples were analyzed for THg via oxidation with bromine chloride for a minimum of 24 hours, purge and trap, and CVAFS (EPA Method 1631 revision E) on a Tekran 2600 Automated Total Mercury Analyzer. Note that prior to analysis, cloudwater samples were filtered at 0.45 μm to remove insects and particulate black carbon residues. Calibration, CCV, MDL, and MS were performed using Ultra Scientific certified aqueous Hg standard (10 μg/L); QCS and OPR were performed using NIST certified reference material 1641D (Mercury in Water, 1.557 mg/kg). The method detection limit was 0.2 ng/L.

Four of the six method blanks analyzed had THg concentrations below the detection limit; the others had THg concentrations of 0.25 and 0.33 ng/L. In comparison, the lowest THg concentration measured in a sample was 0.41 ng/L, while all other samples had THg concentrations above 1.0 ng/L. Samples were analyzed for MeHg via direct aqueous ethylation with sodium tetraethylborate, purge and trap, and CVAFS (EPA Method 1630, Hammerschmidt and Fitzgerald 2006) on a Tekran 2500 spectrometer. Calibration, CCV, MDL, and OPR were performed using Frontier Geosciences certified laboratory MeHg standards. The method detection limit was 0.02 ng/L. Water samples were analyzed for DOC via persulfate-ultraviolet oxidation (EPA Method 5310C) with a Teledyne Tekmar Apollo organic carbon analyzer and anions (SO_4^{2-}) via ion chromatography (IC) with chemical suppression of eluent conductivity (EPA Method 4110B) with a Dionex ion chromatograph. All quality control results can be found in Supplementary Table A1.

2.5 Flux and Pool Calculations

Precipitation scaling factors were used to calculate open precipitation and throughfall fluxes at each elevation based on elevational scaling factors previously determined for Whiteface Mountain [*Miller et al.*, 1993], according to:

$$SF_P = 0.0746 * (elev) + 51.718 \quad [1]$$

where SF_P is the precipitation scaling factor and elev is the elevation of the plot in meters. Precipitation scaling factors were then multiplied by 2015 Hg concentrations and monthly

precipitation volume from the NADP NTN to calculate monthly THg and MeHg fluxes. To calculate litterfall fluxes at each elevation, 2015 litterfall concentrations were multiplied by the average litterfall mass collected in 2009 and 2010 since 2015 litterfall was measured only for concentrations and not for fluxes.

Cloudwater THg and MeHg fluxes at each elevation were calculated using measured cloudwater Hg concentrations at the summit in an elevational cloudwater model [*Miller et al.*, 1993]. In this model, cloudwater THg and MeHg concentrations at the summit were assumed to represent cloudwater concentrations at other elevations, and the average cloudwater moisture flux employed for calculations in the model was estimated from the average of a ten-year record of annual cloudwater volumes. Scaling factors for each elevation were determined, according to:

$$SF_{CW} = 3 \times 10^{-20} (elev)^{6.9434} \quad [2]$$

where SF_{CW} is the cloudwater moisture flux scaling factor and elev is the elevation of the plot in meters. Cloudwater THg and MeHg concentrations were multiplied by the average cloudwater moisture flux and scaling factor to determine cloudwater THg and MeHg fluxes at each elevation. Total Hg and MeHg fluxes at each elevation were defined as the sum of throughfall, litterfall, and cloudwater inputs.

Organic (Oi/Oe and Oa horizons) soil Hg pools were calculated using the relationship between soil %C and bulk density reported in Huntington et al. (1989):

$$\ln(BD_i) = 0.263 - 0.147 \ln(\%C_i) - 0.103(\ln\%C_i)^2 \quad [3]$$

where BD_i is bulk density. Calculated bulk density values for each sample were then used to determine organic layer Hg pools, according to:

$$SP_i = C_i * BD_i * T \quad [4]$$

where SP_i is the organic soil Hg pool (mg/m^2), C_i is the Hg concentration (ng/g), and T is the horizon thickness (cm). To calculate the average soil pool at Whiteface Mountain, we used an average Oi/Oe horizon thickness of 3 cm for the deciduous and coniferous zones and 2 cm for the alpine zone and an average Oa horizon thickness of 7 cm for the deciduous and coniferous zones and 4 cm for the alpine zone, based on field measurements. Average organic soil Hg pools were calculated as the sum of the average Oi/Oe and Oa horizon Hg pools.

2.6 Statistical Analyses

Statistical analyses were performed using SAS version 9.4 (SAS Institute). When necessary, data were log-transformed before applying statistical analyses to satisfy distributional assumptions. All concentrations below the detection limit were assigned a concentration of 0. Ordinary least square and multivariate regression analyses across the elevational gradient were performed using a general linear model with PROC REG via step-wise regression. Influential datapoints determined using Cook's D and outliers determined as values greater than 3 on the studentized residual plot were removed when performing regression analyses. All model residuals were tested for normality using the Shapiro-Wilk test, homogeneity of variance using

the White test, and autocorrelation using the Durbin-Watson test. Results from regression analyses are reported as trends across the elevational gradient.

Three-way Analysis of Variance (ANOVA) factorial design analyses were performed with PROC GLM Type III sum of squares and Tukey's *post-hoc* adjustment to compare soil concentrations in soil horizons (2 levels), across the growing season (3 levels), and among forest cover types (3 levels). Two-way ANOVA factorial design analyses were performed with PROC GLM Type III sum of squares and Tukey's *post-hoc* adjustment to compare throughfall and open precipitation concentrations and fluxes across the growing season (5 levels) and among forest cover types (3 levels). One-way ANOVA analyses were performed with PROC GLM Type III sum of squares and Tukey's *post-hoc* adjustment to compare between throughfall and open precipitation concentrations (2 levels) and to compare cloudwater, litterfall, and soil Hg fluxes and pools by forest cover type (3 levels). Reported p-values reflect main effect comparisons within factors (H_0 = all means within a factor are equal) at an alpha value of 0.05 and a marginal significance alpha value of 0.1. Comparisons within factors reflect simple effect differences within the factor using Tukey's *post-hoc* adjustment at an alpha value of 0.05. Correlations among variables were performed using PROC CORR and Spearman Rank Correlation coefficients at an alpha value of 0.05. Results from ANOVA analyses are reported as trends by forest cover type.

Based upon our sampling design, sample sizes were as follows: n=216 for soils (n=72 per forest cover type, n=108 per horizon, n=72 per month), n=12 for litterfall (n=4 per forest cover

type), n=57 for throughfall (n=19 per forest cover type, n=12 for August and September, n=11 for all other months), n=15 for precipitation (n=3 per month), and n=22 for cloudwater. Due to limited sample quantities, not all samples were analyzed for all chemical species; sample sizes for statistical analyses were adjusted accordingly, with ANOVA comparisons made using Type III analyses to account for the unbalanced design. Data are presented as the arithmetic mean ± 1 standard error. All reported results referring to elevational trends use values

3. Results

3.1 Atmospheric Deposition: Throughfall, Precipitation, and Cloudwater

Average THg concentration in open precipitation was 8.1 ± 1.9 ng/L, MeHg concentration was 0.047 ± 0.012 ng/L, and percent Hg as MeHg (%MeHg) was 0.64 ± 0.13% (Figure 1). Average throughfall THg concentration was 12.4 ± 0.9 ng/L, MeHg concentration was 0.087 ± 0.019 ng/L, and %MeHg was 0.55 ± 0.085%. Throughfall concentrations were higher than open precipitation for THg and marginally lower for percent Hg as MeHg ($p<0.0001$, $p=0.074$, respectively). However, there was no significant difference in MeHg concentrations between throughfall and open precipitation ($p=0.48$).

Throughfall concentrations on Whiteface varied monthly over the season sampled ($p=0.0001$ for THg, $p=0.011$ for MeHg, $p=0.095$ for %MeHg). Higher concentrations of THg were found in July (15.2 ± 2.3 ng/L) and August (13.9 ± 1.9 ng/L) compared to May (7.7 ± 1.5 ng/L), June (10.4 ± 2.3 ng/L), and September (9.4 ± 1.7 ng/L). Marginally higher concentrations

of MeHg and %MeHg occurred in July (0.13 ± 0.04 ng/L, 0.98 ± 0.30%) compared to the other months (mean range of 0.026 to 0.077 ng/L, mean range of 0.21 to 0.84%, respectively). Throughfall THg concentration also varied by forest cover type ($p<0.0001$), with the highest values found in the coniferous zone (15.7 ± 1.8 ng/L), followed by the alpine zone (13.3 ± 1.1 ng/L), and the lowest concentration found in the deciduous zone (8.3 ± 1.1 ng/L; Figure 1). There was no significant difference by forest cover type for throughfall concentrations of MeHg ($p=0.31$; 0.082 ± 0.028 ng/L in the alpine zone, 0.086 ± 0.022 ng/L in the coniferous zone, and 0.092 ± 0.046 ng/L in the deciduous zone) and %MeHg ($p=0.31$; 0.64 ± 0.19%, 0.67 ± 0.15%, 0.36 ± 0.10%, respectively).

Cloudwater concentrations were measured at the summit of Whiteface. The average THg cloudwater concentration was 4.3 ± 0.5 ng/L, with a range of 1.8 ng/L to 9.9 ng/L. The average MeHg cloudwater concentration was 0.023 ± 0.003 ng/L, with a range of 0.013 ng/L to 0.073 ng/L.

Sulfate and DOC concentrations in throughfall also exhibited marginal spatial patterns ($p=0.090$, $p=0.060$, respectively). Average throughfall SO_4^{2-} concentration was 295 ± 35 μg S/L across Whiteface. Marginally higher SO_4^{2-} concentrations were found in the alpine zone (385 ± 80 μg S/L) compared to the coniferous (260 ± 51 μg S/L) and deciduous zones (234 ± 30 μg S/L). Average growing season SO_4^{2-} throughfall flux was 3.5 ± 0.3 g/m^2. Sulfate flux also differed by forest cover type ($p=0.0268$), with highest growing season SO_4^{2-} flux found in the coniferous zone (44 ± 6 μg S/m^2) compared to the deciduous (31 ± 4 μg S/m^2) and alpine zones

(28 ± 5 μg S/m^2). Average throughfall DOC concentration was 9.2 ± 1.2 mg C/L across Whiteface. Marginally higher DOC concentrations were found in the alpine (12.6 ± 2.8 mg C/L) and coniferous zones (11.5 ± 1.8 mg C/L) compared to the deciduous zone (7.6 ± 1.8 mg C/L).

3.2 Mercury in Litterfall

Mercury concentrations in litterfall varied by forest cover type for THg concentrations ($p<0.0001$) and varied marginally for MeHg concentrations and %MeHg ($p=0.083$, $p=0.0924$, respectively; Figure 2). For THg, concentrations were highest in the alpine zone (67 ± 3.9 ng/g), followed by the coniferous zone (48 ± 3.9 ng/g), and lowest in the deciduous zone (31 ± 1.4 ng/g). For MeHg, concentrations were highest in the coniferous zone (0.052 ± 0.0060 ng/g), followed by the alpine zone (0.039 ± 0.0049 ng/g), and lowest in the deciduous zone (0.031 ± 0.0071 ng/g). For %MeHg, values were highest in the coniferous (0.10 ± 0.0063%) and deciduous zones (0.10 ± 0.021%), and lowest in the alpine zone (0.061 ± 0.0081%). Additionally, THg concentration in litter was positively correlated with elevation ($p<0.0001$), and %MeHg in litter was negatively correlated with elevation ($p=0.075$).

3.3 Mercury in Soil

Organic soil concentrations of THg and MeHg showed spatial variations on Whiteface ($p<0.0001$ for both THg and MeHg; Figure 3). The pattern by forest cover type differed for THg and MeHg for the combined organic horizons. Total Hg concentrations were greatest in the

alpine (337 ± 16 ng/g) and coniferous zones (298 ± 15 ng/g) compared to the deciduous zone (156 ± 8 ng/g). Methyl Hg concentrations were highest in the coniferous zone (0.39 ± 0.068 ng/g) compared to the alpine (0.28 ± 0.042 ng/g) and deciduous zones (0.17 ± 0.022 ng/g; Figure 3).

Variation between organic soil horizons (Oi/Oe, Oa) showed similar patterns for THg, MeHg, and %MeHg, with higher values found in the Oa horizon ($p<0.0001$ for THg, $p=0.023$ for MeHg, $p=0.017$ for %MeHg; Figure A2). The Oa horizon also displayed higher THg/C ($p<0.0001$) and THg/N ratios ($p<0.0001$) than the Oi/Oe horizon. The Oa horizon had a mean THg concentration of 313 ± 14 ng/g compared to 209 ± 8 ng/g for the Oi/Oe horizon, mean MeHg concentration of 0.30 ± 0.029 ng/g compared to 0.18 ± 0.026 ng/g for the Oi/Oe horizon, and mean %MeHg value of 0.12 ± 0.015% compared to 0.07 ± 0.010% for the Oi/Oe horizon. On average, the Oa horizon had 1.5 times greater THg concentration, 1.7 times greater MeHg concentration, and 1.2 times greater %MeHg than the Oi/Oe horizon.

Several elevational patterns were evident for soil Hg concentrations across Whiteface. Soil THg concentrations increased with elevation ($p<0.0001$, $r^2=0.39$ for Oi/Oe horizon; $p<0.0001$, $r^2=0.48$ for Oa horizon; $p<0.0001$, $r^2=0.38$ for combined model containing Oi/Oe and Oa horizons), while %MeHg values decreased with elevation ($p=0.0002$, $r^2=0.17$ for Oa horizon; $p=0.081$, $r^2=0.060$ for Oi/Oe horizon; $p<0.0001$, $r^2=0.12$ for combined model). No elevational patterns were found for MeHg concentrations ($p=0.16$), likely due to peak values occurring in the mid-elevation coniferous zone.

Soil THg, MeHg, and %MeHg also displayed seasonal variations on Whiteface ($p=0.074$, $p<0.0001$, $p=0.019$, respectively), with the highest values occurring in July (Figure 4). Total Hg concentrations in the alpine zone, MeHg concentration in the alpine and deciduous zones, and %MeHg in the alpine and deciduous zones were lower in June than July. Lower THg concentrations, MeHg concentrations, and %MeHg in the alpine and deciduous zone occurred in September compared to July.

3.4 Soil Chemical Properties in Relation to Mercury

The average soil C/N ratio at Whiteface was 21 ± 0.3 g C/g N. Ratios of C/N varied by forest cover type ($p<0.0001$), with highest values in the coniferous zone (23 ± 0.4 g C/g N) compared to the deciduous (20 ± 0.5 g C/g N) and alpine zones (21 ± 0.4 g C/g N, Figure 3). In the alpine zone, average C/N ratios decreased from 42 ± 2 g C/g N in the litter to 21 ± 3 g C/g N in the Oi/Oe and Oa horizons, representing a 49% decrease. In the coniferous zone, average C/N ratios decreased from 46 ± 8 g C/g N in the litter to 22 ± 3 g C/g N in the soil, respectively, representing a 52% decrease. In the deciduous zone, average C/N ratios decreased from 50 ± 17 g C/g N in the litter to 20 ± 4 g C/g N in the soil, respectively, representing a 60% decrease. Soil C/N June ratios were marginally higher than July and September ($p=0.055$). The average soil S concentration was 1.9 ± 0.05 mg S/g. Concentrations of S also varied by forest cover type ($p=0.032$), with highest values in the alpine (1.9 ± 0.09 mg S/g) and coniferous zones (2.0 ± 0.09 mg S/g) compared to the deciduous zone (1.6 ± 0.09 mg S/g).

The soil ratios of THg/C and THg/N displayed spatial variation ($p<0.0001$ for THg/C and THg/N; Figure 3), with highest Hg/C ratios in the coniferous and alpine zones compared to the deciduous zone and THg/N ratios highest in the coniferous and alpine zones compared to the deciduous zone. The THg/C ratios increased with elevation ($p<0.0001$, $r^2=0.11$), as did C/N ratios ($p=0.0032$, $r^2=0.04$). The ratio of THg/C increased from the litter to the Oa horizon. In the alpine zone, average THg/C ratios increased from 1.25 ± 0.07 μg/g in the litter to 6.0 ± 0.4 μg/g in the Oi/Oe horizon to 11.0 ± 0.5 μg/g in the Oa horizons, representing an 880% increase. In the coniferous zone, average THg/C ratios increased from 0.88 ± 0.08 μg/g to 4.8 ± 0.3 μg/g to 11.0 ± 0.5 μg/g, respectively, representing a 1300% increase. In the deciduous zone, average THg/C ratios increased from 0.64 ± 0.03 μg/g to 4.5 ± 0.7 μg/g to 7.1 ± 0.5 μg/g, respectively, representing a 1100% increase. Additionally, soil MeHg concentrations were positively correlated with the ratio of THg/C ($p<0.0001$, $r^2=0.3252$), as well as the ratio of THg/N ($p<0.0001$, $r^2=0.3048$). Percent MeHg was marginally negatively correlated with S concentrations in soils ($p=0.081$, $r^2=0.1294$) and marginally positively correlated with the ratio of THg/C ($p=0.093$, $r^2=0.1184$).

Using multivariate linear regression, soil MeHg concentrations on Whiteface were best predicted by S concentrations; though this relationship was marginally significant ($p=0.064$), it only explained 3.2% of the variability in observed soil MeHg concentrations. Soil THg concentrations were best predicted by a model that included elevation, C, N, and S

concentrations ($p<0.0001$, $r^2=0.45$). Soil %MeHg values were best predicted by a model that included THg and C concentrations ($p<0.0001$, $r^2=0.30$).

3.5 Terrestrial Mercury Fluxes

Average growing season open precipitation Hg flux for all forest cover types was 7.3 ± 0.3 μg/m^2 for THg and 38 ± 12 ng/m^2 for MeHg. Methyl Hg open precipitation fluxes exhibited much greater variation than THg fluxes. Average monthly growing season open precipitation THg and MeHg fluxes did not vary by forest cover type ($p=0.21$, $p=0.1685$, respectively; Figure 5). Conversely, average THg open precipitation flux for all forest cover types showed marginal spatial variation by forest cover type across the entire growing season ($p=0.065$). Average THg open precipitation flux for all forest cover types also showed seasonal variation with the highest fluxes in June (4.4 ± 2.6 μg/m^2) compared to the other months (range of 0.44 to 0.98 μg/m^2). Average MeHg open precipitation flux for all forest cover types did not vary by month ($p=0.35$).

Average growing season throughfall Hg fluxes for all forest cover types were highly variable, with fluxes of 8.5 ± 0.7 μg/m^2 for THg and 50 ± 11 ng/m^2 for MeHg. Methyl Hg throughfall fluxes had much greater variation than THg fluxes. Average growing season throughfall THg fluxes varied by forest cover type and month ($p<0.0001$ for both), with highest fluxes in the alpine (10 ± 0.7 μg/m^2) and coniferous zones (11 ± 1 μg/m^2), compared to the deciduous zone (4.5 ± 0.7 μg/m^2; Figure 5). Total Hg throughfall flux averaged for all forest cover types was highest in June and July (2.0 ± 0.3 μg/m^2 and 2.5 ± 0.3 μg/m^2, respectively)

compared to the other months (range of 1.1 to 1.6 μg/m^2 for May, August, September, and October). Average growing season throughfall MeHg flux did not vary by forest cover type ($p=0.38$) or by month ($p=0.18$).

Average modeled growing season cloudwater THg flux was 4.3 ± 0.9 μg/m^2. Modeled growing season cloudwater THg flux increased with elevation (as per the model structure) and varied by forest cover type ($p<0.0001$; Figure 5). The highest modeled growing season cloudwater THg flux was found in the alpine zone (9.7 ± 0.3 μg/m^2), followed by the coniferous zone (3.1 ± 0.4 μg/m^2), and lowest in the deciduous zone (0.07 ± 0.02 μg/m^2). Average modeled growing season cloudwater MeHg flux was 23 ± 3.0 ng/m^2. Modeled growing season cloudwater MeHg flux increased with elevation (as per the model structure) and varied by forest cover type ($p<0.0001$; Figure 5). The highest modeled growing season cloudwater MeHg flux was found in the alpine zone (52 ± 2 ng/m^2), followed by the coniferous zone (17 ± 2 ng/m^2), and lowest in the deciduous zone (0.40 ± 0.09 ng/m^2).

Average litterfall flux was 7.0 ± 0.8 μg/m^2 THg and 6.0 ± 1.3 ng/m^2 MeHg. Total Hg litterfall fluxes did not display any significant patterns by forest cover type ($p=0.17$) or elevation ($p=0.14$), whereas MeHg litterfall flux varied among forest cover types ($p=0.0363$; Figure 5). The highest litterfall MeHg flux occurred in the deciduous zone (8.1 ± 2.1 ng/m^2), followed by the coniferous zone (7.3 ± 1.1 ng/m^2), and was lowest in the alpine zone (2.9 ± 0.5 ng/m^2). Consequently, MeHg litterfall fluxes decreased with elevation ($p=0.022$ and $r^2=0.23$).

Across all forest cover types on Whiteface Mountain, average growing season total flux (litterfall + throughfall + cloudwater) was 18 ± 3 $\mu g/m^2$ for THg and was 80 ± 11 ng/m^2 for MeHg. The relative contribution of litterfall inputs to total flux was 35% for THg and 7% for MeHg, relative contribution of throughfall inputs was 43% for THg and 64% for MeHg, and relative contribution of cloudwater inputs was 22% for THg and 29% for MeHg.

3.6 *Organic Mercury Soil Pools*

Average THg and MeHg organic soil pools across the mountain varied by soil horizon ($p<0.0001$ for both) and forest cover type ($p<0.0001$, $p=0.034$, respectively; Figure 5). Average THg and MeHg organic soil pools were greater in the Oa horizon (4100 ± 250 $\mu g/m^2$, 5.4 ± 1.5 $\mu g/m^2$, respectively) compared to the Oi/Oe horizon (970 ± 20 $\mu g/m^2$, 1.0 ± 0.3 $\mu g/m^2$, respectively). Total Hg organic soil pools were greatest in the coniferous zone (6100 ± 300 $\mu g/m^2$) compared to the deciduous (4100 ± 200 $\mu g/m^2$) and alpine zones (4000 ± 200 $\mu g/m^2$). Methyl Hg organic soil pools were also greatest in the coniferous zone (8.4 ± 1.9 $\mu g/m^2$) compared to the alpine (3.6 ± 0.6 $\mu g/m^2$) and deciduous zones (6.2 ± 1.1 $\mu g/m^2$). Methyl Hg organic soil pools also differed by season, with the highest values found in July ($p<0.0001$).

4. Discussion

4.1 Overall Soil Hg Patterns

Several distinct patterns of soil Hg concentrations were found with elevation and forest cover type. Both elevation and forest cover type can act to control spatial patterns in soils Hg and MeHg. Some mechanisms are controlled solely by forest cover type (e.g., litterfall), while in other instances, both elevation and forest cover type act together to control soil Hg dynamics (e.g., throughfall, soil geochemistry). Blackwell and Driscoll (2015) observed that soil THg concentrations increased with elevation from the deciduous to alpine zone along Whiteface Mountain, which is comparable to patterns reported for other montane studies of Hg [*Fisher and Wolfe*, 2012; *Stankwitz et al.*, 2012; *Townsend et al.*, 2014] and other contaminants introduced to forested ecosystems by atmospheric deposition [*Lovett and Kinsman*, 1990; *Miller et al.*, 1993]. In contrast, soil MeHg concentrations did not exhibit a continuous increasing pattern with elevation, as values were highest in the coniferous zone. This finding is consistent with other forest studies that have reported higher MeHg concentrations in coniferous soils compared to deciduous soils [*Witt et al.*, 2009], though we are not aware of studies that have compared MeHg concentrations along a montane elevational gradient. We found that soil %MeHg patterns were inconsistent with spatial MeHg concentration patterns, as %MeHg decreased along the elevational gradient. The magnitude of observed THg and MeHg concentrations, as well as %MeHg values, in organic soils are consistent with those reported in the literature [e.g., *Grigal*, 2002, 2003; *Obrist*, 2012].

Both THg and MeHg concentrations in soils were higher in the Oa horizon compared to the Oi/Oe horizon. This soil horizon pattern is consistent with some studies in both natural and

manipulated forested ecosystems [*Obrist et al.*, 2011, 2012; *Juillerat et al.*, 2012]. However, some other studies have shown THg and MeHg concentrations to be highest in the Oi/Oe horizon [*Demers et al.*, 2007; *Hojdová et al.*, 2007]. Higher concentrations of MeHg in the Oa horizon likely reflect vertical percolation and retention of precipitation-derived THg and MeHg [*Jiskra et al.*, 2014], as well as the greater extent of organic matter decomposition compared to the Oi/Oe horizon; as organic matter decomposes, mineralized ionic Hg is available for microbial conversion to MeHg [*Obrist et al.*, 2011]. Moreover, the Oa horizon might be more prone to microsites of reducing conditions, which would facilitate the production of MeHg.

4.2 Atmospheric Deposition as a Driver of MeHg Concentrations in Soils

Direct inputs of MeHg concentrations from atmospheric deposition can influence MeHg concentrations and %MeHg within soils [*Hojdová et al.*, 2007; *Witt et al.*, 2009]. Though atmospherically deposited Hg can be reemitted (evaded) or transported (i.e., through surface runoff), the majority is believed to be sequestered within soils [*Driscoll et al.*, 2007]. Atmospheric deposition has been shown to be an important source of THg to terrestrial ecosystems [*Grigal*, 2002], but much less is known about the importance of atmospheric deposition as a source of MeHg.

At Whiteface, spatial patterns in soil MeHg concentrations do not appear to be driven by MeHg in atmospheric deposition. Methyl Hg in precipitation can originate from direct emissions and transport of MeHg, abiotic atmospheric oxidative processes that convert RGM to MeHg,

and/or soil evasion [*Conaway et al.*, 2010; *Fu et al.*, 2010]. However, these processes are thought to be quantitatively insignificant, and thus atmospheric deposition of MeHg is expected to be small [*Bloom and Watras*, 1989]. Accordingly, %MeHg values in wet deposition were <1% of THg at Whiteface, similar to other montane Hg studies [*Conaway et al.*, 2010; *Fu et al.*, 2010]. The lack of an elevational or forest cover pattern for precipitation MeHg concentrations suggests that wet MeHg concentrations are consistent across the mountain, though wet deposition MeHg flux is higher in the coniferous and alpine zones due to greater precipitation quantity. Interestingly, this lack of spatial pattern in MeHg concentrations is inconsistent with the elevational pattern of THg concentrations in precipitation, which increases with elevation. Other studies have suggested that MeHg concentrations in wet deposition are independent of THg and are instead dependent upon atmospheric methylation processes and concentration of atmospheric methylating agents, both of which are limited [*Lee and Iverfeldt*, 1991; *Hammerschmidt et al.*, 2007].

Atmospheric deposition of Hg to mountains also occurs via cloudwater. Due to orographic effects, cloudwater contributions of Hg can result in higher Hg deposition at higher elevations [*Fisher and Wolfe*, 2012]. Some studies have found that THg deposition from clouds at high elevations can be twice that of wet deposition [*Dore et al.*, 1999; *Lawson et al.*, 2003]. The impact of cloudwater on Hg deposition is particularly important in the coniferous and alpine zones of mountains; at these higher elevations, the base of the cloud, which contains the highest solute concentration, can contribute high levels of deposition via contact with leaf surfaces

[*Lovett and Kinsman*, 1990]. At Whiteface, the summit has been estimated to be covered by clouds for 40-45% of the year, with significant cloud coverage also found in the coniferous zone [*Mohnen*, 1988]. Consequently, previous studies have found cloudwater contribution to THg deposition at Whiteface to be the most important input of Hg to the alpine zone and a comparable input to throughfall Hg deposition in the coniferous zone [*Blackwell and Driscoll*, 2015]. We also find cloudwater to be an important contributor in alpine and coniferous zones. Similar cloudwater depositional patterns are apparent for MeHg, with important inputs of cloudwater MeHg flux occurring in the alpine and coniferous zones. These results suggest the importance of characterizing cloudwater Hg when quantifying depositional and storage pathways in montane ecosystems.

Another potential source of atmospheric Hg input to soils is dry deposition, which is represented by Hg in throughfall and litterfall. Reactive gaseous Hg and PHg can adsorb to foliage through dry deposition; Hg is then leached by precipitation as throughfall [*Lindberg et al.*, 1995]. Throughfall inputs of THg have been shown to be 1.5 to 1.8 times that of open precipitation due to the wash-off of Hg from leaves [*Choi et al.*, 2008]. Additionally, conifers are more efficient at filtering atmospheric Hg particles than deciduous trees due to greater surface roughness, high leaf area index, and a canopy structure that decreases air flow and thereby enhances particle adsorption [*Kolka et al.*, 1999; *Rea et al.*, 2002; *Johnson et al.*, 2007; *Witt et al.*, 2009]. As a result, THg inputs via throughfall are typically the predominant source of THg to coniferous forests [*Demers et al.*, 2007], which is consistent with our results and previous

work at Whiteface [*Blackwell and Driscoll*, 2015]. Throughfall inputs of THg to alpine zones, however, are reduced due to lower total leaf area associated with sparse tree density and lower canopy height. Though differences in throughfall THg concentrations for coniferous and deciduous forests have been shown, MeHg concentration patterns exhibit mixed results [*Graydon et al.*, 2008]. The source of MeHg in throughfall could be either dry deposition of atmospheric MeHg or methylation of RGM to MeHg on foliar surfaces [*Graydon et al.,* 2008]. We did not find any difference in throughfall MeHg concentrations among forest cover types or across the elevational gradient at Whiteface. Additionally, throughfall MeHg concentrations at Whiteface were not different than open precipitation MeHg concentrations, suggesting minimal MeHg adsorption onto leaf surfaces or foliar surface production and/or minimal losses of adsorbed and produced foliar MeHg in throughfall. Inconsistent results have been reported in the literature, with some studies noting similar findings to us of no significant difference between MeHg in throughfall and open precipitation [*Lee and Iverfeldt*, 1991; *Munthe et al.*, 1995; *Johnson et al.*, 2007], while others have observed higher MeHg concentrations in throughfall [*Witt et al.,* 2009]. Throughfall inputs do not appear to contribute to forest cover type patterns of MeHg concentration at Whiteface.

The final source of atmospheric MeHg inputs to terrestrial ecosystems is litterfall, which we found to exhibit a similar spatial pattern to that observed in soil MeHg concentrations. Other studies have also found litterfall to be a major input of both THg and MeHg to forested ecosystems, with 30-70% of THg inputs to forests originating from litterfall [*Munthe et al.*,

1995; *Rea et al.*, 1996, 2002; *Hall and St. Louis*, 2004; *Demers et al.*, 2007; *Graydon et al.*, 2008]. Total Hg in litterfall is derived from atmospheric inputs of GEM through direct uptake by stomata [*Rea et al.*, 2000, 2002; *Rutter et al.*, 2011; *Risch et al.*, 2012] as trees absorb atmospheric and locally evaded Hg [*Rea et al.*, 1996]. Conifers are particularly effective at scavenging Hg compared to deciduous trees because of the multi-year lifespan of needles [*Mowat et al.*, 2011; *Fisher and Wolfe*, 2012], which is consistent with our finding at Whiteface of greater THg concentrations in coniferous litterfall compared to deciduous litterfall. Since Hg accumulates in foliage throughout the growing season, litterfall is an important source of THg inputs to forests [*Bushey et al.*, 2008]. Though atmospheric inputs are a small fraction of the forest floor THg pool, these new inputs of THg are likely more biologically available than older THg stored within the soil and therefore more readily methylated [*Hintelmann et al.*, 2002; *Grigal*, 2003]. Additionally, we found that MeHg concentrations in litterfall were highest in the coniferous zone. In contrast, MeHg litterfall flux was highest in the deciduous zone, mirroring the pattern of %MeHg in soils. The source of MeHg in litter is unclear, but it could be derived either from uptake of MeHg by leaves through the stomata or methylation of Hg on the foliar surface.

Though landscape patterns are apparent in MeHg deposition concentrations (litterfall) and fluxes (throughfall, open precipitation, cloudwater, and litterfall), the magnitude of these inputs are much smaller than the MeHg soil pool (Figure 5). The ratio of growing season total MeHg inputs prorated for the year to MeHg soil pool is 0.016 ± 0.002 yr^{-1} for the deciduous

zone, 0.034 ± 0.007 yr^{-1} for the coniferous zone, and 0.14 ± 0.02 yr^{-1} for the alpine zone; these ratios are similar to that of growing season total THg inputs prorated for the year to THg soil pool (0.0096 ± 0.0005 yr^{-1}, 0.010 ± 0.005 yr^{-1}, 0.023 ± 0.001 yr^{-1}, respectively). Thus, because annual atmospheric MeHg deposition is a small fraction of the forest floor MeHg pool, it is unlikely to be an important driver of MeHg concentrations in soils.

4.3 Internal Drivers of MeHg Formation in Soils

We propose that soil microbial methylation of ionic Hg to MeHg is the primary source of MeHg in soils. The activity of methylating prokaryotes in terrestrial ecosystems can be driven by labile organic matter, SO_4^{2-} supply, environmental conditions (i.e., redox conditions, temperature), and the concentration and bioavailability of THg [*Gilmour et al.*, 1992; *Warner et al.*, 2005; *Watras et al.*, 2005].

The activity of many methylators is dependent upon labile C and SO_4^{2-} in soils for the metabolic process that results in the production of MeHg [*Grigal*, 2003; *Shanley and Bishop*, 2012]. Litterfall, root turnover, exudates, and the organic horizon in soils provide organic C for bacteria [*Grigal*, 2003; *Amirbahman and Fernandez*, 2012], with higher elevation forests containing a greater organic C pool than lower elevation forests [*Bolstad and Vose*, 2001]. However, previous research has found no effect of C concentrations on MeHg concentrations [*Hojdová et al.*, 2007]. At the same time, several studies have also noted the importance of S concentrations in soils for controlling Hg methylation pathways [*Steffan et al.*, 1988; *Shanley*

and Bishop, 2012]. Inputs of SO_4^{2-} in precipitation and throughfall have been shown to increase across an elevational gradient in montane ecosystems, including Whiteface [*Lovett and Kinsman*, 1990; *Miller et al.*, 1993]. Our results support this finding, with highest SO_4^{2-} concentrations in wet deposition occurring in the alpine zone and highest SO_4^{2-} fluxes occurring in the coniferous zone. Accordingly, at Whiteface, the S concentration in organic soils was greatest in the coniferous and alpine zones. Though we found S concentration in soils to be the most important factor for predicting MeHg concentrations across Whiteface, with the peak MeHg concentration occurring in the coniferous zone, soil S concentrations explained only a small percent of the variability in soil MeHg concentrations. Moreover, the highest %MeHg values, considered to be an indicator of methylation activity, were found in the deciduous zone where atmospheric SO_4^{2-} deposition and soil S concentrations are relatively low. Microbial utilization of SO_4^{2-} is thus likely not the major limiting controller of the activity of methylating prokaryotes.

Increased anoxic conditions (associated with soil saturation) and increased temperature enhance methylation activity [*Morel et al.*, 1998; *Ullrich et al.*, 2001; *Grigal*, 2003; *Amirbahman and Fernandez*, 2012]. Such dependence of methylation on environmental conditions was evident from seasonal patterns at Whiteface, with highest MeHg soil concentrations found in July when temperatures were warmer and increased precipitation contributed to wetter soils (Figure A3). Spatially, the dependence of methylators on temperature and reducing conditions was also apparent. Warmer temperatures at lower elevations likely explain the higher production of MeHg (and resulting higher %MeHg) in the deciduous zone and lower MeHg concentrations

in the alpine zone compared to the coniferous zone. Seasonality in MeHg soil concentrations also suggests the role of demethylation. During the early summer, from June to July, soil MeHg concentrations and pools increase, likely as methylation of Hg increases with increasing temperature. Conversely, during the late summer, from July to September, soil MeHg concentrations and pools decrease, as decreases in temperature (Figure A3) likely decrease methylation rates or as demethylation increases in response to the earlier increases in methylation. Thus, it appears that the soil MeHg pool and elevational patterns at Whiteface are driven by the temperature-dependence of microbial activity.

Total Hg bioavailability, which is derived from the mineralization of soil organic matter (SOM) degradation, is also a potentially important controller of methylation activity. Higher rates of SOM decomposition, manifested as lower C/N ratios [*Obrist et al.*, 2011], can lead to higher MeHg concentrations in soils. We found the deciduous zone to have the lowest C/N ratios and greatest percent changes in C/N ratios between the litter and organic soil layers compared to the coniferous and alpine zones. This pattern in C/N soil ratios among forest cover types suggests higher rates of SOM mineralization and thus increased THg bioavailability in the deciduous zone. In turn, bioavailable THg is likely more readily methylated by microbial processes in the deciduous zone, which is further supported by the higher %MeHg. This pattern in THg bioavailability differs from THg concentrations, which are highest in the alpine zone.

Although the supply of bioavailable THg appears to be more efficiently methylated in the warmer deciduous zone with its greater mineralization of SOM, the greater concentrations of

THg in organic soils of the coniferous and alpine zones apparently drive the higher concentrations of soil MeHg, albeit less efficiently, in these upper elevations compared to the lower elevation deciduous zone. Our analysis suggests that spatial variation in MeHg concentrations in the montane ecosystem are primarily driven by inputs and soil concentrations of THg, but this pattern is secondarily altered by the warmer temperature and lability of SOM in the deciduous zone, which allows for more efficient methylation than the colder coniferous and alpine zones.

4.4 Implications of Soil MeHg Patterns

This assessment of MeHg patterns in deposition and soils across a montane environment may allow for a greater understanding of Hg cycling in terrestrial ecosystems. The finding of decreasing %MeHg with elevation might suggest that Hg concentrations in biota should be highest in the deciduous zone. However, in an assessment of Bicknell's thrush (*Catharus bicknelli*), Swainson's thrush (*Catharus ustulatus*), and Hermit thrush (*Catharus guttatus*) across the deciduous and coniferous zones of Whiteface, Hg blood concentrations increased with elevation, with coniferous zone concentrations nearly twice that of the deciduous zone [*Driscoll and Sauer*, 2015]. Similar findings have been found at other mountains for thrushes and salamanders [*Townsend et al.*, 2014]. Thus, songbird Hg concentrations appear to follow patterns in absolute soil MeHg concentration, not relative soil MeHg concentration (%MeHg), and absolute soil MeHg concentrations may be a better indicator of wildlife exposure to MeHg.

Moreover, previous studies have reported correlations between regional patterns of Hg flux patterns and Bicknell's thrush blood Hg and have accordingly suggested high bioavailability of terrestrial MeHg [*Rimmer et al.*, 2005]. The relationship between soil MeHg concentrations and songbird blood Hg concentrations at Whiteface helps corroborate these speculations. Since birds can display physiological, behavioral, and reproductive effects from high Hg concentrations and are bioindicators of MeHg bioavailability for many species, it is important to understand and reduce exposure of MeHg to these species by understanding external and internal drivers of MeHg in terrestrial environments [*Rimmer et al.*, 2005; *Evers et al.*, 2007].

At Whiteface Mountain, a montane forested environment, MeHg concentrations appear to be driven predominantly by internal processing of Hg by methylating organisms. With Hg loading 2-5x higher in montane northeastern forests such as the Adirondacks compared to lower elevations and other regions [*Miller et al.*, 2005; *Rimmer et al.*, 2005], this study provides an improved understanding of Hg drivers in high elevation biological Hg hotspots. In addition to elevated Hg deposition, alpine wildlife are likely highly susceptible to the effects of climate change. Regulations such as the Mercury and Air Toxics Standard that decrease Hg deposition (and thereby MeHg concentrations) [*Gerson and Driscoll*, 2016; *Zhou et al.*, 2017] in montane ecosystems could lead to reductions in avian blood Hg concentration and reduce stress to vulnerable populations.

Acknowledgements

We thank J. Dukett, K. Alberga, P. Casson, R. Brandt, the Department of Environmental Conservation (DEC), and the New York State Olympic Regional Development Authority (ORDA) for allowing access to sites and for fieldwork assistance; D. Gay and L. Zhang for assistance in calculating deposition fluxes; and K. Murray for revisions on the manuscript. We also thank the group of graduate and undergraduate students who assisted in field collection and laboratory analyses. Finally, we appreciate the suggestions and comments provided by three anonymous reviewers to improve the analysis in this manuscript. The data associated with this study can be obtained from the Forest Ecosystem Monitoring Cooperative data archive (https://www.uvm.edu/femc/data/archive/project/biological-mercury-hotspots-montane-ecosystems-northern-forest).

This project was funded by a grant from the Northeastern States Research Cooperative (NSRC) through funding made available by the USDA Forest Service and the New York State Energy and Research Development Authority (NYSERDA). J Gerson received funding from a Syracuse University Graduate Fellowship, American Association of University Women (AAUW) Selected Professions Fellowship, and American Water Resources Associations (AWRA) Richard A. Herbert Memorial Scholarship. The conclusions and opinions in this paper are those of the authors and do not reflect those of the NSRC, the Forest Service, USDA, AAUW, or AWRA. Any use of trade, firm, or product names is for descriptive purposes only and does not imply endorsement by the U.S. Government.

Figures

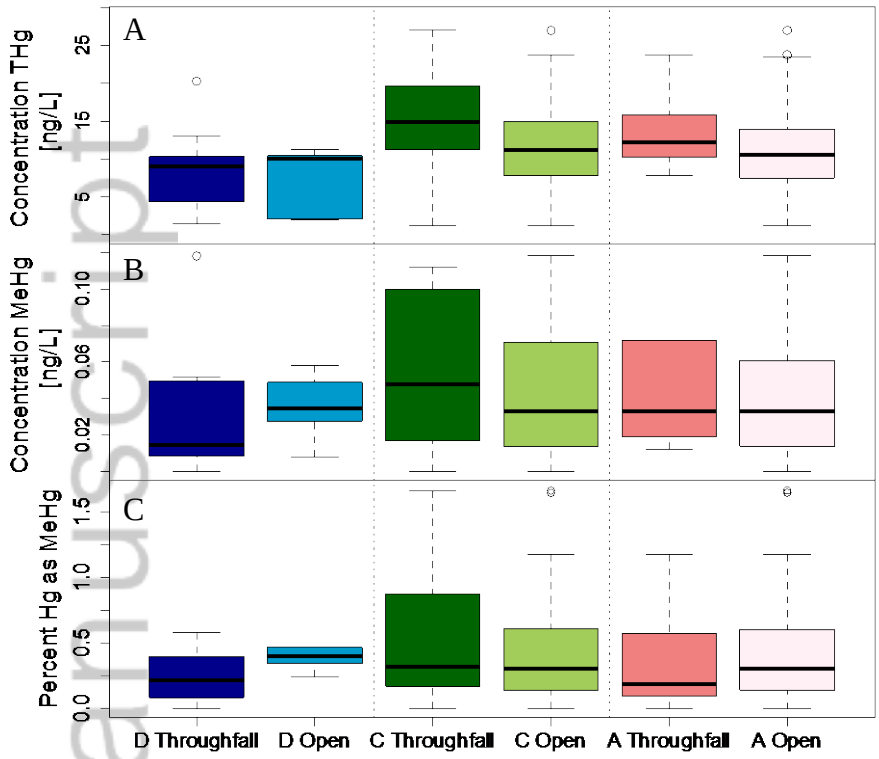

Figure 1: Concentrations of A) total mercury, B) methylmercury, and C) percent mercury as methylmercury in wet deposition (throughfall and open precipitation) across different forest cover types at Whiteface Mountain (D represents deciduous, C represents coniferous, and A represents alpine). Box-and-whisker plots show median values, Q1, and Q3 within the boxes, and the whiskers represent Q1 - 1.5*interquartile range and Q3 + 1.5*interquartile range (n=19 for throughfall at each forest cover type, n=5 for open precipitation at each forest cover type). Only outliers within the given bounds are shown.

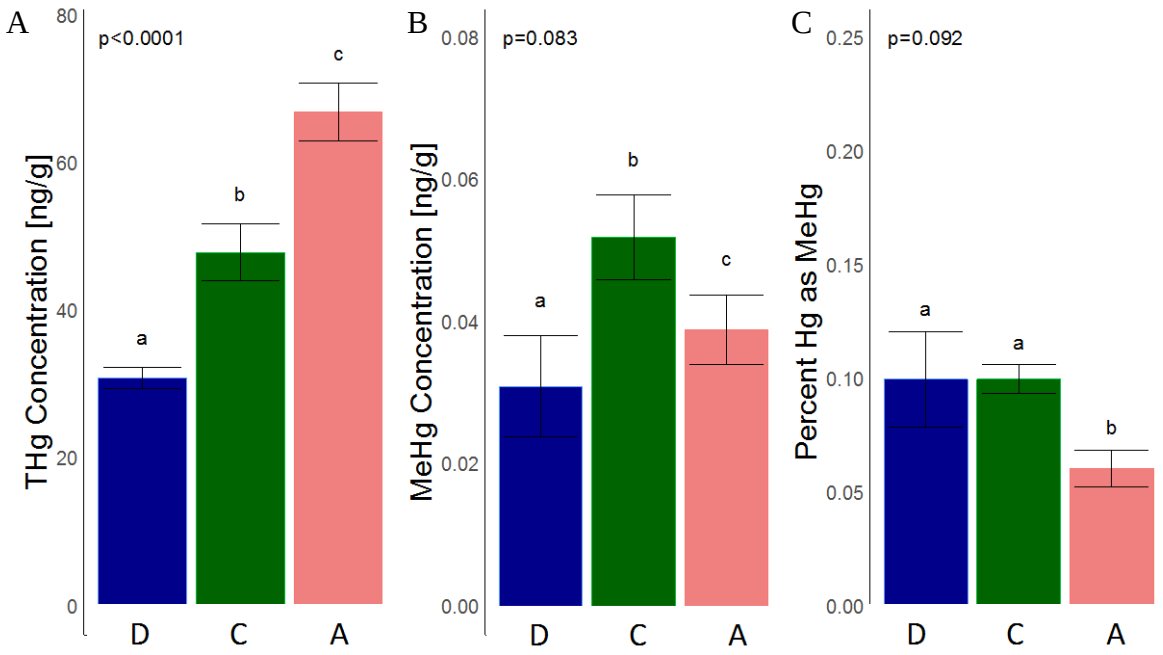

Figure 2: Concentrations of litterfall A) total mercury, B) methylmercury, and C) percent mercury as methylmercury across different forest cover types at Whiteface Mountain (D represents deciduous, C represents coniferous, and A represents alpine). Barplots show mean values, and error bars denote standard error (n=4 for each forest cover type). Reported p-values represent differences between all levels (H_0 = means for all forest cover types are equal). Letters denote significant differences using Tukey's *post-hoc* adjustment at an alpha level of 0.05.

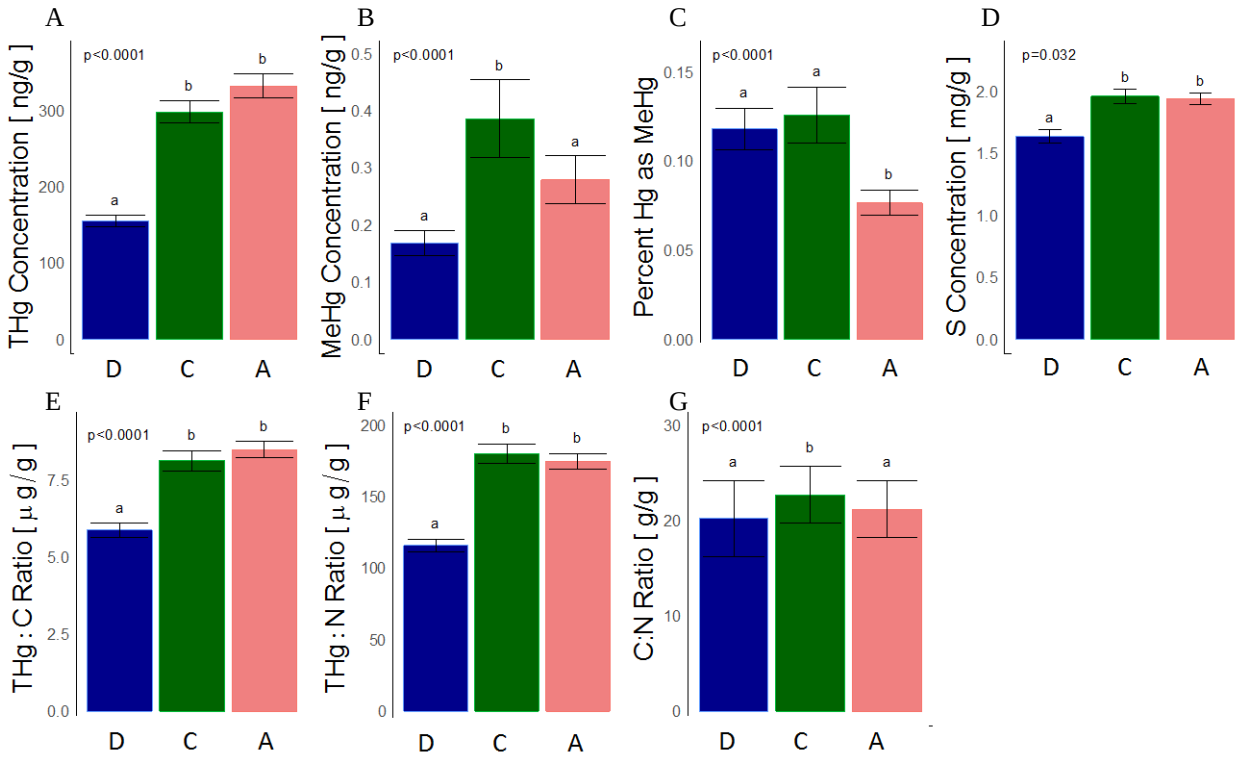

Figure 3: Organic soil mercury and ancillary characteristics across different forest cover types at Whiteface Mountain: A) total mercury, B) methylmercury, C) percent mercury as methylmercury, D) percent sulfur, E) total mercury: percent carbon ratio, F) total mercury: percent nitrogen ratio, G) percent carbon: percent nitrogen ratio. Barplots show mean values, and error bars denote standard errors (n=72 for each forest cover type). Reported p-values represent differences between all levels (H_0 = means for all forest cover types are equal). Letters denote significant differences using Tukey's *post-hoc* adjustment at an alpha level of 0.05.

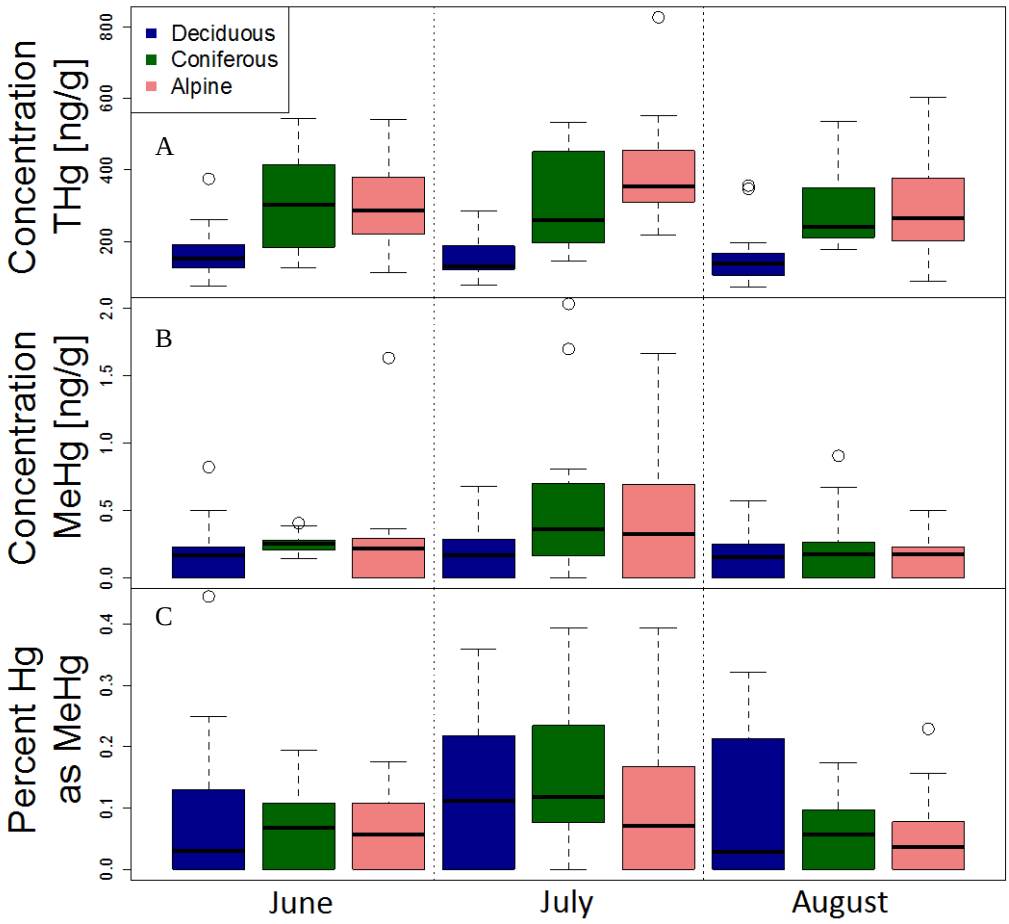

Figure 4: Concentrations of A) total mercury, B) methylmercury, and C) percent mercury as methylmercury in organic soils across the growing season at different forest cover types at Whiteface Mountain. Box-and-whisker plots show median values, Q1, and Q3 within the boxes, and the whiskers represent Q1 - 1.5*interquartile range and Q3 + 1.5*interquartile range (n=24 for each forest cover type in each month). Only outliers within the given bounds are shown.

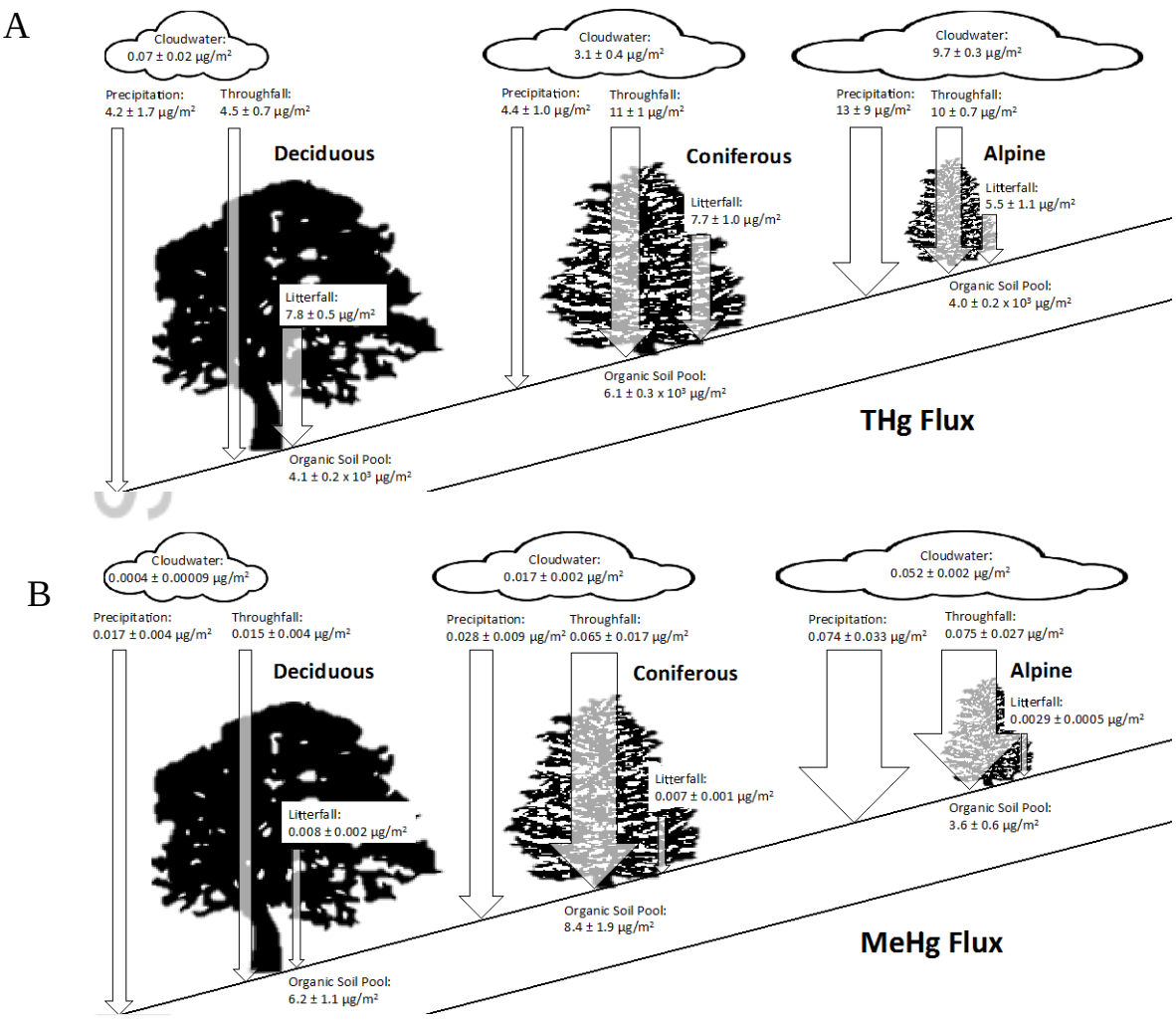

Figure 5: Comparison of growing season (May-September) A) total mercury and B) methylmercury fluxes and organic soil pools in different forest cover types at Whiteface Mountain. Values denote mean and standard error (calculated by propagating errors in mercury concentration).

References

Amirbahman, A., and I. J. Fernandez (2012), The role of soils in storage and cycling of mercury, in *Mercury in the environment: Pattern and process*, edited by M. S. Bank, pp. 99–118, University of California Press, Berkeley, CA.

Blackwell, B. D., and C. T. Driscoll (2015), Deposition of mercury in forests along a montane elevation gradient, *Environ. Sci. Technol.*, *49*(9), 5363–5370, doi:10.1021/es505928w.

Blackwell, B. D., C. T. Driscoll, J. A. Maxwell, and T. M. Holsen (2014), Changing climate alters inputs and pathways of mercury deposition to forested ecosystems, *Biogeochemistry*, *119*, 215–228, doi:10.1007/s10533-014-9961-6.

Blais, J. M., S. Charpentié, F. Pick, L. E. Kimpe, A. S. Amand, and C. Regnault-Roger (2006), Mercury, polybrominated diphenyl ether, organochlorine pesticide, and polychlorinated biphenyl concentrations in fish from lakes along an elevation transect in the French Pyrénées, *Ecotoxicol. Environ. Saf.*, *63*, 91–99, doi:10.1016/j.ecoenv.2005.08.008.

Bloom, N. S., and C. J. Watras (1989), Observations of methylmercury in precipitation, *Sci. Total Environ.*, *87–88*, 199–207, doi:10.1016/0048-9697(89)90235-0.

Bolstad, P., and J. Vose (2001), The effects of terrain position and elevation on soil C in the southern Appalachians, in *Assessment Methods for soil carbon*, edited by R. Lal, pp. 4–51, Lewis Publishers, Boca Raton, FL.

Bushey, J. T., A. G. Nallana, M. R. Montesdeoca, and C. T. Driscoll (2008), Mercury dynamics of a northern hardwood canopy, *Atmos. Environ.*, *42*(29), 6905–6914,

doi:10.1016/j.atmosenv.2008.05.043.

Choi, H. D., T. J. Sharac, and T. M. Holsen (2008), Mercury deposition in the Adirondacks: A comparison between precipitation and throughfall, *Atmos. Environ.*, *42*(8), 1818–1827, doi:10.1016/j.atmosenv.2007.11.036.

Compeau, G. C., and R. Bartha (1985), Sulfate-reducing bacteria: Principal methylators of mercury in anoxic estuarine sediment, *Microbiology*, *50*(2), 498–502.

Conaway, C. H., F. J. Black, P. Weiss-Penzias, M. Gault-Ringold, and A. R. Flegal (2010), Mercury speciation in Pacific coastal rainwater, Monterey Bay, California, *Atmos. Environ.*, *44*(14), 1788–1797, doi:10.1016/j.atmosenv.2010.01.021.

Dellinger, J., M. Dellinger, and J. S. Yauck (2012), Mercury exposures in vulnerable populations: Guidelines for fish consumption, in *Mercury in the environment: Pattern and process*, edited by M. Bank, pp. 289–301, University of California Press, Berkeley, CA.

Demers, J. D., C. T. Driscoll, T. J. Fahey, and J. B. Yavitt (2007), Mercury cycling in litter and soil in different forest types in the Adirondack region, New York, USA, *Ecol. Appl.*, *17*(5), 1341–1351.

Demers, J. D., J. D. Blum, and D. R. Zak (2013), Mercury isotopes in a forested ecosystem : Implications for air-surface exchange dynamics and the global mercury cycle, *Global Biogeochem. Cycles*, *27*, 222–238, doi:10.1002/gbc.20021.

Dore, A., M. Sobik, and K. Migala (1999), Patterns of precipitation and pollutant deposition in the western Sudete mountains, Poland, *Atmos. Environ.*, *33*, 3301–3312,

doi:10.1016/S1352-2310(98)00294-5.

Driscoll, C., and A. Sauer (2015), *Methylmercury bioaccumulation within terrestrial food webs in the Adirondack Park of New York State*, NYSERDA Report 16-06.

Driscoll, C. T., Y.-J. Han, C. Y. Chen, D. C. Evers, K. F. Lambert, T. M. Holsen, N. C. Kamman, and R. K. Munson (2007), Mercury contamination in forest and freshwater ecosystems in the northeastern United States, *Bioscience*, *57*(1), 17, doi:10.1641/B570106.

Driscoll, C. T., R. P. Mason, H. M. Chan, D. J. Jacob, and N. Pirrone (2013), Mercury as a global pollutant: Sources, pathways, and effects, *Environ. Sci. Technol.*, *47*, 4967–4983.

Dukett, J. E., N. Aleksic, N. Houck, P. Snyder, P. Casson, and M. Cantwell (2011), Progress toward clean cloud water at Whiteface Mountain New York, *Atmos. Environ.*, *45*(37), 6669–6673, doi:10.1016/j.atmosenv.2011.08.070.

Evers, D. C., Y.-J. Han, C. T. Driscoll, N. C. Kamman, M. W. Goodale, K. F. Lambert, T. M. Holsen, C. Y. Chen, T. A. Clair, and T. Butler (2007), Biological mercury hotspots in the northeastern United States and southeastern Canada, *Bioscience*, *57*(1), 29–43, doi:10.1641/B570107.

Fisher, L. S., and M. H. Wolfe (2012), Examination of mercury inputs by throughfall and litterfall in the Great Smoky Mountains National Park, *Atmos. Environ.*, *47*, 554–559, doi:10.1016/j.atmosenv.2011.10.017.

Fitzgerald, W. F., D. R. Engstrom, R. P. Mason, and E. A. Nater (1998), The case for atmospheric mercury contamination in remote areas, *Environ. Sci. Technol.*, *32*(1), 1–7,

doi:10.1021/es970284w.

Fu, X. W., X. Feng, Z. Q. Dong, R. S. Yin, J. X. Wang, Z. R. Yang, and H. Zhang (2010), Atmospheric gaseous elemental mercury (GEM) concentrations and mercury depositions at a high-altitude mountain peak in south China, *Atmos. Chem. Phys.*, *10*(5), 2425–2437, doi:10.5194/acp-10-2425-2010.

Gerson, J. R., and C. T. Driscoll (2016), Is mercury in a remote forested watershed of the Adirondack Mountains responding to recent decreases in emissions?, *Environ. Sci. Technol.*, *50*(20), 10943–10950, doi:10.1021/acs.est.6b02127.

Gilmour, C. C., E. A. Henry, and R. Mitchell (1992), Sulfate Stimulation of mercury methylation in freshwater sediments, *Environ. Sci. Technol.*, *26*(3), 2281–2287, doi:10.1021/es00035a029.

Gilmour, C. C., M. Podar, A. L. Bullock, A. M. Graham, S. D. Brown, A. C. Somenahally, A. Johs, R. A. Hurt, K. L. Bailey, and D. A. Elias (2013), Mercury methylation by novel microorganisms from new environments, *Environ. Sci. Technol.*, *47*(20), 11810–11820, doi:10.1021/es403075t.

Graydon, J. A., V. L. St. Louis, H. Hintelmann, S. E. Lindberg, K. A. Sandilands, J. W. M. Rudd, C. A. Kelly, B. D. Hall, and L. D. Mowat (2008), Long-term wet and dry deposition of total and methyl mercury in the remote boreal ecoregion of Canada, *Environ. Sci. Technol.*, *42*(22), 8345–8351, doi:10.1021/es801056j.

Grigal, D. F. (2002), Inputs and outputs of mercury from terrestrial watersheds: A review,

Environ. Rev., *10*(1), 1–39, doi:10.1139/a01-013.

Grigal, D. F. (2003), Mercury sequestration in forests and peatlands *J. Environ.* a review, *Qual.*, *32*, 393–405.

Hall, B. D., and V. L. St. Louis (2004), Methylmercury and total mercury in plant litter decomposing in upland forests and flooded landscapes, *Environ. Sci. Technol.*, *38*(19), 5010–5021, doi:10.1021/es049800q.

Hammerschmidt, C. R., and W. F. Fitzgerald (2006), Photodecomposition of methylmercury in an arctic Alaskan lake, *Environ. Sci. Technol.*, *40*(4), 1212–1216.

Hammerschmidt, C. R., C. H. Lamborg, and W. F. Fitzgerald (2007), Aqueous phase methylation as a potential source of methylmercury in wet deposition, *Atmos. Environ.*, *41*(8), 1663–1668, doi:10.1016/j.atmosenv.2006.10.032.

Hintelmann, H., and H. T. Nguyen (2005), Extraction of methylmercury from tissue and plant samples by acid leaching, *Anal. Bioanal. Chem.*, *381*(2), 360–365, doi:10.1007/s00216-004-2878-5.

Hintelmann, H., R. Harris, A. Heyes, J. P. Hurley, C. A. Kelly, D. P. Krabbenhoft, S. Lindberg, J. W. M. Rudd, K. J. Scott, and V. L. St. Louis (2002), Reactivity and mobility of new and old mercury deposition in a boreal forest ecosystem during the first year of the METAALICUS study, *Environ. Sci. Technol.*, *36*(23), 5034–5040, doi:10.1021/es025572t.

Hojdová, M., J. H. Huang, K. Kalbitz, and E. Matzner (2007), Effects of throughfall and litterfall manipulation on concentrations of methylmercury and mercury in forest-floor percolates, *J.*

Plant Nutr. Soil Sci., *170*(3), 373–377, doi:10.1002/jpln.200622023.

Jiskra, M., D. Saile, J. G. Wiederhold, B. Bourdon, E. Björn, and R. Kretzschmar (2014), Kinetics of Hg(II) exchange between organic ligands, goethite, and natural organic matter studied with an enriched stable isotope approach, *Environ. Sci. Technol.*, *48*(22), 13207–13217, doi:10.1021/es503483m.

Johnson, K. B., T. A. Haines, J. S. Kahl, S. A. Norton, A. Amirbahman, and K. D. Sheehan (2007), Controls on mercury and methylmercury deposition for two watersheds in Acadia National Park, Maine, *Environ. Monit. Assess.*, *126*, 55–67, doi:10.1007/s10661-006-9331-5.

Juillerat, J. I., D. S. Ross, and M. S. Bank (2012), Mercury in litterfall and upper soil horizons in forested ecosystems in Vermont, USA, *Environ. Toxicol. Chem.*, *31*(8), 1720–1729, doi:10.1002/etc.1896.

Kerin, E. J., C. C. Gilmour, E. Roden, M. T. Suzuki, J. D. Coates, and R. P. Mason (2006), Mercury methylation by dissimilatory iron-reducing bacteria, *Appl. Environ. Microbiol.*, *72*(12), 7919–7921, doi:10.1128/AEM.01602-06.

Kolka, R. K., E. A. Nater, D. F. Grigal, and E. S. Verry (1999), Atmospheric inputs of mercury and organic carbon into a forested upland/bog watershed, *Water. Air. Soil Pollut.*, *113*, 273–294, doi:10.1023/A:1005020326683.

Lawson, S. T., T. D. Scherbatskoy, E. G. Malcolm, and G. J. Keeler (2003), Cloud water and throughfall deposition of mercury and trace elements in a high elevation spruce-fir forest at

Mt. Mansfield, Vermont, *J. Environ. Monit.*, *5*, 578–583, doi:10.1039/b210125d.

Lee, Y.-H., and A. Iverfeldt (1991), Measurement of methylmercury and mercury in run-off, lake and rain waters, *Water, Air Soil Pollut.*, *56*, 309–321, doi:10.1017/CBO9781107415324.004.

Lindberg, S. E., K. H. Kim, T. P. Meyers, and J. G. Owens (1995), Micrometeorological gradient approach for quantifying air/surface exchange of mercury vapor: Tests over contaminated soils, *Environ. Sci. Technol.*, *29*, 126–135, doi:10.1021/es00001a016.

Lorey, P., and C. T. Driscoll (1999), Historical trends of mercury deposition in Adirondack lakes, *Environ. Sci. Technol.*, *33*(5), 718–722, doi:10.1021/es9800277.

Lovett, G. M., and J. D. Kinsman (1990), Atmospheric pollutant deposition to high-elevation ecosystems, *Atmos. Environ.*, *24A*(11), 2767–2786, doi:10.1016/0960-1686(90)90164-I.

Lovett, G. M., and S. E. Lindberg (1984), Dry Deposition and Canopy Exchange in a Mixed Oak Forest As Determined By Analysis of Throughfall, *J. Appl. Ecol.*, *21*(3), 1013–1027, doi:10.2307/2405064.

Miller, E. K., A. J. Friedland, E. A. Arons, V. A. Mohnen, J. J. Battles, J. A. Panek, J. Kadlecek, and A. H. Johnson (1993), Atmospheric deposition to forests along an elevational gradient at Whiteface Mountain, NY, U.S.A., *Atmos. Environ.*, *27A*(14), 2121–2136, doi:10.1016/0960-1686(93)90042-W.

Miller, E. K., A. Vanarsdale, G. J. Keeler, A. Chalmers, L. Poissant, N. C. Kamman, and R. Brulotte (2005), Estimation and mapping of wet and dry mercury deposition across

northeastern North America, *Ecotoxicology*, *14*, 53–70, doi:10.1007/s10646-004-6259-9.

Mohnen, V. A. (1988), Exposure of forests to air pollutants, clouds, precipitation and climatic variables., *EPA-600/3-89-003*, U.S. EPA, Research Triangle Park, N.C.

Morel, F. M. M., A. M. L. Kraepiel, and M. Amyot (1998), The Chemical cycle and bioaccumulation of mercury, *Annu. Rev. Ecol. Syst.*, *29*, 543–566, doi:10.1146/annurev.ecolsys.29.1.543.

Mowat, L. D., V. L. St. Louis, J. A. Graydon, and I. Lehnherr (2011), Influence of forest canopies on the deposition of methylmercury to boreal ecosystem watersheds, *Environ. Sci. Technol.*, *45*(12), 5178–5185, doi:10.1021/es104377y.

Munthe, J., H. Hultberg, and A. Iverfeldt (1995), Mechanisms of deposition of methylmercury and mercury to coniferous forests, *Water. Air. Soil Pollut.*, *80*, 363–371.

Obrist, D. (2012), Mercury distribution across 14 U.S. forests. Part II: Patterns of methyl mercury concentrations and areal mass of total and methyl mercury, *Environ. Sci. Technol.*, *46*(11), 5921–5930, doi:10.1021/es2045579.

Obrist, D. et al. (2011), Mercury distribution across 14 U.S. Forests. Part I: Spatial patterns of concentrations in biomass, litter, and soils, *Environ. Sci. Technol.*, *45*(9), 3974–3981, doi:10.1021/es104384m.

Obrist, D., D. W. Johnson, and R. L. Edmonds (2012), Effects of vegetation type on mercury concentrations and pools in two adjacent coniferous and deciduous forests, *J. Plant Nutr. Soil Sci.*, *175*, 68–77, doi:10.1002/jpln.201000415.

Podar, M., C. C. Gilmour, C. C. Brandt, A. Soren, S. D. Brown, B. R. Crable, A. V Palumbo, A. C. Somenahally, and D. A. Elias (2015), Global prevalence and distribution of genes and microorganisms involved in mercury methylation, *Sci. Adv.*, *1*(9), 1–13, doi:10.1126/sciadv.1500675.

Rahman, M., and H. Kingston (2005), Development of a microwave-assisted extraction method and isotopic validation of mercury species in soils and sediments, *J. Anal. At. Spectrom.*, *20*, 183–191.

Rea, A. W., G. J. Keeler, and T. Scherbatskoy (1996), The deposition of mercury in throughfall and litterfall in the Lake Champlain watershed: A short-term study, *Atmos. Environ.*, *30*(19), 3257–3263, doi:10.1016/1352-2310(96)00087-8.

Rea, A. W., S. E. Lindberg, and G. J. Keeler (2000), Assessment of dry deposition and foliar leaching of mercury and selected trace elements based on washed foliar and surrogate surfaces, *Environ. Sci. Technol.*, *34*(12), 2418–2425, doi:10.1021/es991305k.

Rea, A. W., S. E. Lindberg, and G. J. Keeler (2001), Dry deposition and foliar leaching of mercury and selected trace elements in deciduous forest throughfall, *Atmos. Environ.*, *35*, 3453–3462.

Rea, A. W., S. E. Lindberg, T. Scherbatskoy, and G. J. Keeler (2002), Mercury accumulation in foliage over time in two northern mixed-hardwood forests, *Water. Air. Soil Pollut.*, *133*, 49–67, doi:10.1023/A:1012919731598.

Reiners, W. A., R. H. Marks, and P. M. Vitousek (1975), Heavy metals in subalpine and alpine

soils of New Hampshire, *Oikos*, *26*(3), 264–275.

Rimmer, C. C., K. P. Mcfarland, D. C. Evers, E. K. Miller, Y. Aubry, D. Busby, and R. J. Taylor (2005), Mercury concentrations in Bicknell's thrush and other insectivorous passerines in montane forests of northeastern North America, *Ecotoxicology*, *14*, 223–240.

Rimmer, C. C., E. K. Miller, K. P. McFarland, R. J. Taylor, and S. D. Faccio (2010), Mercury bioaccumulation and trophic transfer in the terrestrial food web of a montane forest, *Ecotoxicology*, *19*, 697–709, doi:10.1007/s10646-009-0443-x.

Risch, M. R., J. F. DeWild, D. P. Krabbenhoft, R. K. Kolka, and L. Zhang (2012), Litterfall mercury dry deposition in the eastern USA, *Environ. Pollut.*, *161*, 284–290, doi:10.1016/j.envpol.2011.06.005.

Rutter, A. P., J. J. Schauer, M. M. Shafer, J. E. Creswell, M. R. Olson, M. Robinson, R. M. Collins, A. M. Parman, T. L. Katzman, and J. L. Mallek (2011), Dry deposition of gaseous elemental mercury to plants and soils using mercury stable isotopes in a controlled environment, *Atmos. Environ.*, *45*(4), 848–855, doi:10.1016/j.atmosenv.2010.11.025.

Shanley, J. B., and K. H. Bishop (2012), Mercury cycling in terrestrial watersheds, in *Mercury in the environment: Pattern and process*, edited by M. Bank, pp. 119–141, University of California Press, Berkeley, CA.

Stankwitz, C., J. M. Kaste, and A. J. Friedland (2012), Threshold increases in soil lead and mercury from tropospheric deposition across an elevational gradient, *Environ. Sci. Technol.*, *46*(15), 8061–8068, doi:10.1021/es204208w.

Steffan, R. J., E. T. Korthals, and M. R. Winfrey (1988), Effects of acidification on mercury methylation, demethylation, and volatilization in sediments from an acid-susceptible lake, *Appl. Environ. Microbiol.*, *54*(8), 2003–2009, doi:10.1023/A:1005972708616.

Townsend, J. M., C. T. Driscoll, C. C. Rimmer, and K. P. Mcfarland (2014), Avian, salamander, and forest floor mercury concentrations increase with elevation in a terrestrial ecosystem, *Environ. Toxicol. Chem.*, *33*(1), 208–215, doi:10.1002/etc.2438.

Tseng, C. M., A. De Diego, F. M. Martin, O. F. X. Donard, A. De Diego, F. M. Martin, and O. F. X. Donard (1997), Rapid and quantitative microwaveassisted recovery of methylmercury from standard reference sediments, *J. Anal. At. Spectrom.*, *12*(6), 629–635, doi:10.1039/a700832e.

Ullrich, S. M., T. W. Tanton, and S. A. Abdrashitova (2001), Mercury in the aquatic environment: A review of factors affecting methylation, *Crit. Rev. Environ. Sci. Technol.*, *31*(3), 241–293, doi:10.1080/20016491089226.

Warner, K. A., J. C. J. Bonzongo, E. E. Roden, G. M. Ward, A. C. Green, I. Chaubey, W. B. Lyons, and D. A. Arrington (2005), Effect of watershed parameters on mercury distribution in different environmental compartments in the Mobile Alabama River Basin, USA, *Sci. Total Environ.*, *347*, 187–207, doi:10.1016/j.scitotenv.2004.12.011.

Watras, C. J., K. A. Morrison, A. Kent, N. Price, O. Regnell, C. Eckley, H. Hintelmann, and T. Hubacher (2005), Sources of methylmercury to a wetland-dominated lake in northern Wisconsin, *Environ. Sci. Technol.*, *39*(13), 4747–4758, doi:10.1021/es040561g.

Witt, E. L., R. K. Kolka, E. A. Nater, and T. R. Wickman (2009), Influence of the forest canopy on total and methyl mercury deposition in the boreal forest, *Water. Air. Soil Pollut., 199*, 3–11, doi:10.1007/s11270-008-9854-1.

Yu, R. Q., I. Adatto, M. R. Montesdeoca, C. T. Driscoll, M. E. Hines, and T. Barkay (2010), Mercury methylation in Sphagnum moss mats and its association with sulfate-reducing bacteria in an acidic Adirondack forest lake wetland, *FEMS Microbiol. Ecol., 74*(3), 655–668, doi:10.1111/j.1574-6941.2010.00978.x.

Yu, X., C. T. Driscoll, M. Montesdeoca, D. Evers, M. Duron, K. Williams, N. Schoch, and N. C. Kamman (2011), Spatial patterns of mercury in biota of Adirondack, New York lakes, *Ecotoxicology, 20*, 1543–1554, doi:10.1007/s10646-011-0717-y.

Yu, X., C. T. Driscoll, R. A. F. Warby, M. Montesdeoca, and C. E. Johnson (2014), Soil mercury and its response to atmospheric mercury deposition across the northeastern United States, *Ecol. Appl., 24*(4), 812–822, doi:10.1890/13-0212.1.

Zhou, H., C. Zhou, M. M. Lynam, J. T. Dvonch, J. A. Barres, P. K. Hopke, M. Cohen, and T. M. Holsen (2017), Atmospheric mercury temporal trends in the northeastern United States from 1992 to 2014: Are measured concentrations responding to decreasing regional emissions?, *Environ. Sci. Technol. Lett.*, In press, doi:10.1021/acs.estlett.6b00452.